Chiral three-nucleon forces and pairing in nuclei

T. Lesinski,[1, 2, *] K. Hebeler,[3, 4, †] T. Duguet,[5, 6, ‡] and A. Schwenk[7, 8, §]

[1]*Department of Physics and Institute for Nuclear Theory,*
University of Washington, Seattle, WA 98195, USA
[2]*Department of Physics and Astronomy, University of Tennessee, Knoxville, TN 37996, USA*
and Physics Division, Oak Ridge National Laboratory, Oak Ridge, TN 37831, USA
[3]*Department of Physics, The Ohio State University, Columbus, OH 43210, USA*
[4]*TRIUMF, 4004 Wesbrook Mall, Vancouver, BC, V6T 2A3, Canada*
[5]*CEA, Centre de Saclay, IRFU/Service de Physique Nucléaire, F-91191 Gif-sur-Yvette, France*
[6]*National Superconducting Cyclotron Laboratory and Department of Physics and Astronomy,*
Michigan State University, East Lansing, MI 48824, USA
[7]*ExtreMe Matter Institute EMMI, GSI Helmholtzzentrum für Schwerionenforschung GmbH, 64291 Darmstadt, Germany*
[8]*Institut für Kernphysik, Technische Universität Darmstadt, 64289 Darmstadt, Germany*

We present the first study of pairing in nuclei including three-nucleon forces. We perform systematic calculations of the odd-even mass staggering generated using a microscopic pairing interaction at first order in chiral low-momentum interactions. Significant repulsive contributions from the leading chiral three-nucleon forces are found. Two- and three-nucleon interactions combined account for approximately 70% of the experimental pairing gaps, which leaves room for self-energy and induced interaction effects that are expected to be overall attractive in nuclei.

With the discovery of BCS theory of superconductivity, it was quickly realized that key nuclear properties, such as the odd-even staggering of binding energies, or moments of inertia having half the rigid-body value, were due to the superfluid nature of nuclei [1]. In fact, pairing has become an essential aspect of nuclear structure, notably for the description of the most proton- and neutron-rich nuclei [2]. Although studies of pairing gaps from internucleon interactions are possible for infinite matter [3–5], they remain a great challenge beyond light nuclei.

For medium-mass and heavy nuclei, the method of choice, especially for systematic global studies, is the nuclear energy density functional (EDF) approach [6]. For a single-reference ground state, pairing is captured through $U(1)$ symmetry breaking and leads to solving effective Hartree-Fock-Bogoliubov (HFB) [7] or Bogoliubov-de Gennes equations. These are solved based on the EDF for both the single-particle and pairing channels. While current EDF parameterizations provide a satisfactory description of low-energy properties of known nuclei, they are empirical in character and lack predictive power as one enters experimentally unexplored regions. It is therefore of great interest to construct non-empirical EDFs derived from microscopic nuclear forces. The development of low-momentum interactions based on renormalization group (RG) methods [8] opens up this possibility.

Describing pairing within a perturbative expansion around the HFB state translates into solving a generalized gap equation. This requires two essential inputs: the normal self-energy that includes interactions between a single nucleon and the medium, together with the anomalous self-energy computed from the pairing interaction kernel. The first-order contribution to the pairing kernel is given directly by two-nucleon (NN) and three-nucleon (3N) forces (where we neglect higher-body interactions), while higher-order terms include induced interactions describing the process of paired particles interacting via the exchange of medium fluctuations. A fundamental, yet unresolved, question is to what extent pairing in nuclei is generated by nuclear forces at first order [9–12], and what is the role of higher-order processes [13–16].

To address this question, we perform a systematic study of pairing gaps generated using a pairing interaction at first order in chiral low-momentum interactions [8]. Building on Refs. [9–11] that explored the contributions from Coulomb and NN interactions only, we include here for the first time 3N forces for pairing in nuclei. Higher-order contributions are left to future works. Since 3N forces play a key role in neutron-rich nuclei [17] and matter in neutron stars [18], this also presents an important step to understanding pairing in neutron stars.

Our calculations start from the N³LO NN potential (EM 500 MeV) of Ref. [19]. This is RG-evolved to low-momentum interactions $V_{\mathrm{low}\,k}$ using a smooth $n_{\mathrm{exp}} = 4$ regulator with $\Lambda = 1.8-2.8\,\mathrm{fm}^{-1}$ [20, 21]. In addition, we include the leading N²LO 3N forces based on chiral EFT without explicit Deltas [22]. They consist of a long-range 2π-exchange part V_{c_i}, an intermediate-range 1π-exchange part V_D and a short-range contact interaction V_E:
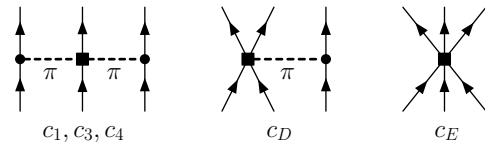
We assume that the c_i coefficients of the long-range 3N parts are not modified by the RG and use the consistent EM c_i's from the NN potential of Ref. [19].

For each cutoff Λ, we take the short-range couplings c_D and c_E from the Faddeev and Faddeev-Yakubovsky fits to the ^{3}H binding energy and the ^{4}He matter radius [23]. This uses a smooth 3N regulator of the form $\exp[-((p^2 + 3/4q^2)/\Lambda_{3NF}^2)^4]$, where p and q are Jacobi momenta. The 3N cutoff Λ_{3NF} is allowed to vary independently of the NN cutoff, which probes the sensitivity to short-range three-body physics. For details and values of the 3N couplings c_i, c_D, c_E, see Ref. [23].

Based on these 3N forces, we construct an antisymmetrized, density-dependent two-body interaction $\overline{V}_{3N}$ by summing one particle over occupied states in the Fermi sea of homogeneous nuclear matter, extending the neutron and symmetric matter calculations of Refs. [23–25] to general isospin asymmetries:

$$\overline{V}_{3N}(k_F^n, k_F^p) = \text{Tr}_{\sigma_3,\tau_3} \int \frac{d\mathbf{k}_3}{(2\pi)^3} \, \theta(k_F^{\tau_3} - |\mathbf{k}_3|) \, \mathcal{A}_{123} \, V_{3N} \,. \tag{1}$$

Here $\mathcal{A}_{123} = 1 - P_{12} - P_{13} - P_{23} + P_{12}P_{23} + P_{13}P_{23}$ denotes the three-body antisymmetrizer, where P_{ij} exchanges spin, isospin and momenta of nucleons i and j. The spin (isospin) projection of the summed particle is denoted by σ_3 (τ_3). For neutron matter, only the c_1 and c_3 parts of 3N forces enter [25], but with protons present, all parts contribute at the density-dependent two-body level. In general, $\overline{V}_{3N}$ depends on the spin, the isospin, the relative momenta $\mathbf{k}, \mathbf{k}'$ and on the total momentum $\mathbf{P}$ of the two interacting particles. However, as shown in Refs. [23, 25], the dependence on $\mathbf{P}$ is very weak and taking $\mathbf{P} = 0$ is a very good approximation.

The density-dependent two-body interaction $\overline{V}_{3N}$ corresponds to the normal-ordered two-body part of 3N forces [25]. Normal ordering with respect to a superfluid HFB state leads to a two-body pairing interaction, where $\overline{V}_{3N}$ is added with a combinatorial factor 1 to the antisymmetrized NN interaction $\overline{V}_{NN} = (1 - P_{12})V_{\text{low }k}$. In this work, we focus on the ^{1}S$_0$ partial-wave contribution that dominates isovector pairing [26], so that the first-order pairing kernel reads

$$\overline{V}_{\text{pairing}}^{^1S_0} = \overline{V}_{NN}^{^1S_0} + \overline{V}_{3N}^{^1S_0} \,. \tag{2}$$

For practical purposes, it is convenient to separate the contributions to $\overline{V}_{3N}$ from the summation over occupied neutron and proton states, $\overline{V}_{3N}(k_F^n, k_F^p) = \overline{V}_{3N,\langle n \rangle}(k_F^n) + \overline{V}_{3N,\langle p \rangle}(k_F^p)$. The strength of the two terms depends on the isospin of the two interacting particles. In Fig. 1, we compare matrix elements of the different 3N contributions to the neutron-neutron ^{1}S$_0$ pairing kernel for two representative densities of symmetric nuclear matter. We find that the 3N contributions are both repulsive, so that pairing will be weaker in nuclei compared to the NN-only level. In addition, $\overline{V}_{3N,\langle p \rangle}^{^1S_0}$ is stronger than $\overline{V}_{3N,\langle n \rangle}^{^1S_0}$, because it involves also isospin $T = 1/2$ triples. These 3N effects can lead to new isospin dependences in pairing gaps.
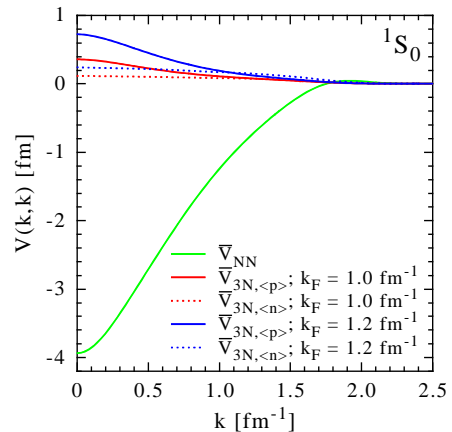

FIG. 1. Antisymmetrized momentum-space matrix elements for low-momentum NN and 3N interactions with $\Lambda/\Lambda_{3NF} = 2.0/2.0 \,\text{fm}^{-1}$ in the neutron-neutron ^{1}S$_0$ channel. The 3N parts are given as density-dependent two-body interactions $\overline{V}_{3N}$ for EM c_i's and c_D, c_E from Ref. [23]. The contributions from summing over neutrons $\langle n \rangle$ and protons $\langle p \rangle$ are shown separately for two Fermi momenta $k_F = 1.0, 1.2 \,\text{fm}^{-1}$ in symmetric nuclear matter. The relative momentum k and the k_F dependence is similar for the other 3N fits of Ref. [23].

In order to perform systematic EDF calculations of semi-magic nuclei, it is convenient to develop an operator representation of $\overline{V}_{3N,\langle \tau \rangle}(k, k'; k_F^\tau)$. We take a rank-$m$ separable Ansatz of the form

$$\overline{V}_{3N,\langle \tau \rangle}^{^1S_0}(k, k'; k_F^\tau) = \sum_{\alpha,\beta=1}^{m} g_\alpha^\tau(k) \, \lambda_{\alpha\beta}^\tau(k_F^\tau) \, g_\beta^\tau(k') \,, \tag{3}$$

with $m \leqslant 4$. The density dependence is parameterized as a polynomial in k_F^τ: $\lambda_{\alpha\beta}^\tau(k_F^\tau) = \sum_{i=3,4} \lambda_{\alpha\beta,i}^\tau (k_F^\tau)^i$. Given our Ansatz, the functions $g_\alpha^\tau(k)$ and the coefficients $\lambda_{\alpha\beta,i}^\tau$ are fitted to the momentum-space matrix elements $\overline{V}_{3N,\langle \tau \rangle}^{^1S_0}(k, k'; k_F^\tau)$ for various values of k_F^τ from 0.6 to $1.6 \,\text{fm}^{-1}$. This describes the matrix elements to better than 0.01 fm. Finally, finite nuclei calculations use the local approximation $\lambda_{\alpha\beta}(k_F^\tau(\mathbf{R}))$ with $k_F^\tau(\mathbf{R}) \equiv (3\pi^2 \rho_\tau(\mathbf{R}))^{1/3}$. We have checked that an alternate choice of local-density dependence based on the Campi-Bouyssy prescription for $k_F^\tau(\mathbf{R})$ [27] leads to pairing gaps within 10 keV of the gaps presented here.

The remaining part of the nuclear EDF, that is due to the normal self-energy and drives the correlated single-particle motion, is taken as a semi-empirical Skyrme parameterization. To be as consistent as possible with the first-order pairing kernel used to compute the anomalous self-energy, the isoscalar and isovector effective masses of the Skyrme parameterization have been constrained from Hartree-Fock results in neutron and symmetric nuclear matter based on low-momentum NN and 3N interactions [28]. The present results do not depend significantly on the Skyrme isoscalar effective mass [29], as long
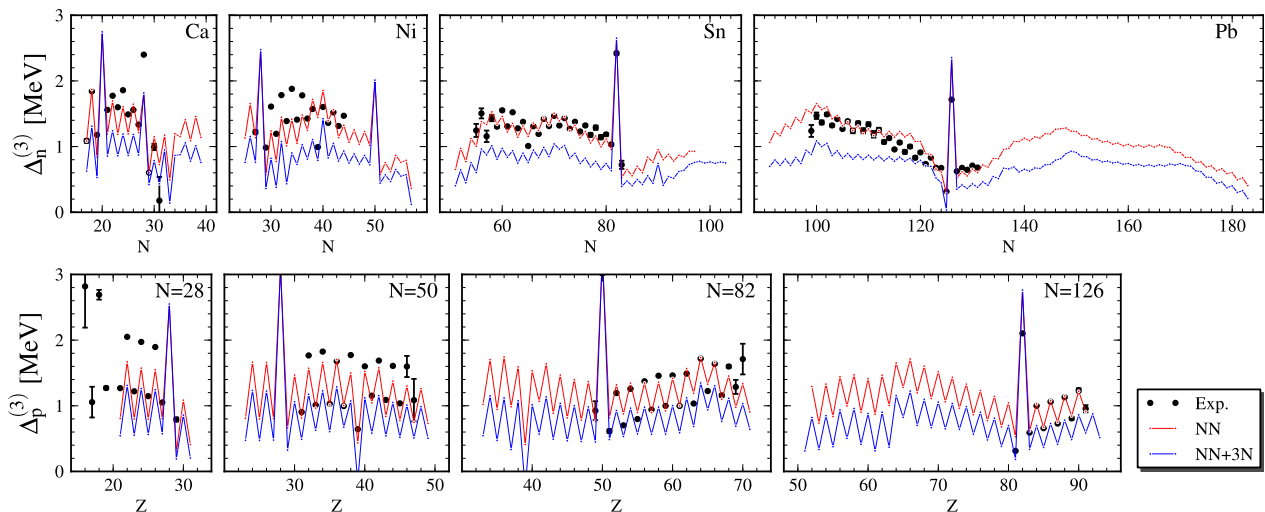
FIG. 2. Theoretical and experimental neutron/proton three-point mass differences $\Delta^{(3)}_{\mathrm{n/p}}$ along isotopic/isotonic chains from one-proton to one-neutron drip-lines based on low-momentum NN and 3N interactions with $\Lambda/\Lambda_{\mathrm{3NF}} = 1.8/2.0 \, \mathrm{fm}^{-1}$. Note that for neutron-rich tin isotopes, the chemical potential is just below threshold such that the one-neutron drip-line is located well before the two-neutron drip-line.

as its value at saturation density is within ≈ 0.67–0.73 as obtained from the microscopic Hartree-Fock calculations.

We use the BSLHFB code [30] that solves the HFB equations in a spherical box of $24\,\mathrm{fm}$ radius, with a mesh size of $0.3\,\mathrm{fm}$. The single-particle wave functions are expanded on a basis of spherical Bessel functions $j_\ell(kr)$ with a momentum cutoff $k_{\mathrm{cut}} = 4.0\,\mathrm{fm}^{-1}$, allowing the description of single-particle states up to energies of about $300\,\mathrm{MeV}$ and ensuring convergence of the pairing gaps to a fraction of a keV.

In this Letter, we focus on the odd-even staggering of nuclear masses that provides a measure of the pairing gap associated with the lack of binding of an odd isotope/isotone relative to its even neighbors. The three-point mass differences are computed in the exact same way from experimental data and EDF calculations. To do so, odd-even nuclei are computed through the self-consistent blocking procedure performed within the filling approximation [11, 31]. In Fig. 2, we present the central results for theoretical and experimental neutron/proton three-point mass differences $\Delta^{(3)}_{\mathrm{n/p}}$ along several semi-magic isotopic/isotonic chains. Results obtained with and without 3N contributions to the first-order pairing interaction kernel are compared.

The main result obtained with NN only is that theoretical neutron and proton pairing gaps computed at lowest order are close to experimental ones for a large set of semi-magic spherical nuclei, although experimental gaps are underestimated in the lightest systems. The addition of the first-order 3N contribution then lowers pairing gaps systematically by about 30%. This is in line with the repulsive $\overline{V}_{\mathrm{3N}}$ in the $^1S_0$ channel (Fig. 1).

Although the impact of the 3N contribution is gener-

ally smooth as a function of (N, Z) and insensitive to the structure of the particular nucleus under consideration, it displays a slight isovector trend. This is seen, e.g., in the lesser reduction of gaps in lead isotopes with $N > 140$ (-30% average relative shift) than $N < 140$ (-35%). Similarly, in the $N = 126$ isotones we find -43% for $Z < 70$ and -35% for $Z > 70$. This effect may be explained by the fact that the interaction involving three neutrons (protons) is less repulsive than the interaction of two neutrons (protons) with a proton (neutron). The resulting density-dependent pairing interaction thus suppresses the neutron (proton) gap less (more) strongly in a neutron-rich, proton-poor nucleus than in a symmetric one.

Next, we study the cutoff dependence of the pairing gaps in Fig. 3. This provides an estimate of the theoretical uncertainties due to short-range higher-order NN and many-body interactions as well as due to an incomplete many-body treatment. To make the comparison clearer, we subtract the oscillating part from the three-point mass differences and consider $\Delta^{(3)} - \overline{\Delta}^{(3)}$, where $\overline{\Delta}^{(3)}$ accounts for that oscillation and is obtained by treating the odd nuclei as if they had the same structure as the even ones [32]. For the large NN cutoff range considered, the pairing gaps at the NN-only level vary by $\approx 100 - 200\,\mathrm{keV}$, and even smaller for less smooth cutoffs. When 3N forces are included, the theoretical uncertainties are of similar size, $\approx 100 - 250\,\mathrm{keV}$, as indicated by the range of dotted and solid lines in Fig. 3. This range includes estimates from neglected shorter-range many-body interactions that are probed when varying the 3N cutoff ($\Lambda_{\mathrm{3NF}} = 2.0 - 2.5\,\mathrm{fm}^{-1}$ for the dotted lines in Fig. 3) and from the uncertainties in the long-range c_i
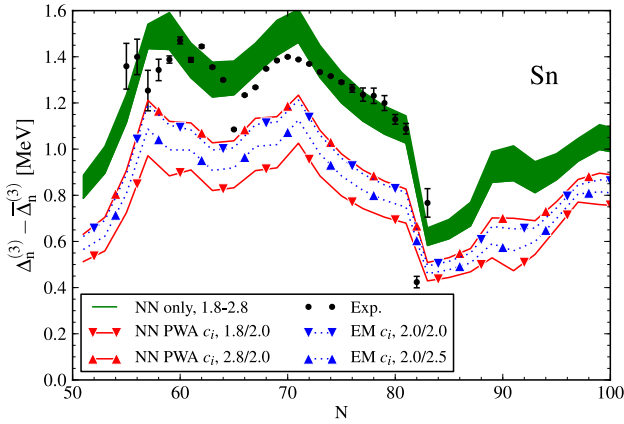
FIG. 3. Cutoff dependence of the three-point mass difference $\Delta_n^{(3)}$ along the tin isotopic chain, with the oscillating part $\overline{\Delta}_n^{(3)}$ subtracted. Results are shown for the NN cutoff range $\Lambda = 1.8 - 2.8\,\mathrm{fm}^{-1}$ (NN-only gaps are the green/solid band) and including 3N forces with different EM/PWA c_i couplings and different NN/3N cutoffs $\Lambda/\Lambda_{3\mathrm{NF}}$ (lines/symbols).

couplings (dotted versus solid lines, where in addition to the consistent EM c_i's, we consider the central c_i values obtained from the NN partial wave analysis (PWA) [33]). For all 3N forces, the short-range couplings c_D, c_E are taken from Ref. [23]. Similar cutoff dependences are found for the other semi-magic chains.

In summary, we have carried out the first study of pairing in nuclei with 3N forces. Our results show that (i) it is essential to include 3N contributions to the pairing interaction for a quantitative description of nuclear pairing gaps, (ii) our first-order low-momentum results leave about 30% room for contributions from higher orders, e.g., from the coupling to (collective) density, spin and isospin fluctuations, consistent with induced interactions being overall attractive in nuclei [13–16], (iii) in the next steps, the normal self-energy and higher-order contributions to the pairing kernel must be computed consistently based on low-momentum NN and 3N interactions. Work in these directions is in progress. Finally, there are indications from phenomenological studies that the quality of the overall agreement between theory and experiment is different for spherical and deformed nuclei [34, 35]. It is therefore of great interest to apply the developed non-empirical pairing energy functional to deformed nuclei.

* E-mail: tlesinsk@uw.edu
† E-mail: hebeler.4@osu.edu
‡ E-mail: thomas.duguet@cea.fr
§ E-mail: schwenk@physik.tu-darmstadt.de

[1] A. Bohr, B. R. Mottelson and D. Pines, Phys. Rev. **110**, 936 (1958).
[2] J. Dobaczewski and W. Nazarewicz, Prog. Theor. Phys. Suppl. **146**, 70 (2003).
[3] D. J. Dean and M. Hjorth-Jensen, Rev. Mod. Phys. **75**, 607 (2003).
[4] A. Schwenk, B. Friman and G. E. Brown, Nucl. Phys. A **713**, 191 (2003).
[5] A. Gezerlis and J. Carlson, Phys. Rev. C **77**, 032801 (2008).
[6] M. Bender, P.-H. Heenen and P.-G. Reinhard, Rev. Mod. Phys. **75**, 121 (2003).
[7] P. Ring and P. Schuck, *The Nuclear Many-Body Problem* (Springer, 1980).
[8] S. K. Bogner, R. J. Furnstahl and A. Schwenk, Prog. Part. Nucl. Phys. **65**, 94 (2010).
[9] T. Duguet and T. Lesinski, Eur. Phys. J. ST **156**, 207 (2008).
[10] T. Lesinski *et al.*, Eur. Phys. J. A **40** 121 (2009).
[11] T. Duguet and T. Lesinski, AIP Conf. Proc. **1165**, 243 (2009).
[12] H. Hergert and R. Roth, Phys. Rev. C **80**, 024312 (2009).
[13] J. Terasaki *et al.*, Nucl. Phys. A **697**, 127 (2002).
[14] F. Barranco *et al.*, Eur. Phys. J. A **21**, 57 (2004).
[15] G. Gori *et al.*, Phys. Rev. C **72**, 1 (2005).
[16] A. Pastore *et al.*, Phys. Rev. C **78**, 024315 (2008).
[17] T. Otsuka *et al.*, Phys. Rev. Lett. **105**, 032501 (2010); J. D. Holt *et al.*, arXiv:1009.5984.
[18] K. Hebeler *et al.*, Phys. Rev. Lett. **105**, 161102 (2010).
[19] D. R. Entem and R. Machleidt, Phys. Rev. C **68**, 041001(R) (2003).
[20] S. K. Bogner *et al.*, Nucl. Phys. A **784**, 79 (2007).
[21] K. Hebeler, A. Schwenk and B. Friman, Phys. Lett. B **648**, 176 (2007).
[22] U. van Kolck, Phys. Rev. C **49**, 2932 (1994); E. Epelbaum *et al.*, Phys. Rev. C **66**, 064001 (2002).
[23] K. Hebeler *et al.*, Phys. Rev. C **83**, 031301(R) (2011).
[24] J. W. Holt, N. Kaiser and W. Weise, Phys. Rev. C **81**, 024002 (2010).
[25] K. Hebeler and A. Schwenk, Phys. Rev. C **82**, 014314 (2010).
[26] S. Baroni, A. O. Macchiavelli and A. Schwenk, Phys. Rev. C **81**, 064308 (2010).
[27] X. Campi and A. Bouyssy, Phys. Lett. B **73**, 263 (1978).
[28] K. Hebeler *et al.*, Phys. Rev. C **80**, 044321 (2009).
[29] T. Lesinski, T. Duguet, K. Bennaceur and J. Meyer, unpublished.
[30] T. Lesinski, Ph.D. Thesis (Université Lyon 1, 2008).
[31] S. Perez-Martin and L. M. Robledo, Phys. Rev. C **78**, 014304 (2008).
[32] T. Duguet *et al.*, Phys. Rev. C **65**, 014311 (2002).
[33] M. C. M. Rentmeester, R. G. E. Timmermans and J. J. de Swart, Phys. Rev. C **67**, 044001 (2003).
[34] G. F. Bertsch *et al.*, Phys. Rev. C **79**, 034306 (2009).
[35] M. Yamagami, Y. R. Shimizu and T. Nakatsukasa, Phys. Rev. C **80**, 064301 (2009).